

Declaration

I, **Sujay Routh**, hereby declare that the present thesis, entitled “**Exploring the Reliability of LDMOS and Junctionless FETs in Harsh Environments: High-Temperature and High-Radiation Applications**”, is the record of work done by me under the supervision of Dr. Ratul Kumar Baruah, Associate Professor, Department of Electronics and Communication Engineering, Tezpur University, Tezpur. The contents of the thesis represent my original works that have not been previously submitted for any Degree/Diploma/Certificate in any other University or Institutions of Higher Education.

This thesis is being submitted to Tezpur University for the Degree of Doctor of Philosophy in Electronics and Communication Engineering.

Place: Tezpur University, Tezpur

Date:

(Sujay Routh)



TEZPUR UNIVERSITY


(A Central University Established by an Act of Parliament)
Napaam, Tezpur-784028, Sonitpur, Assam, India

Certificate

This is to certify that the thesis entitled, “**Exploring the Reliability of LDMOS and Junctionless FETs in Harsh Environments: High-Temperature and High-Radiation Applications**”, submitted to the School of Engineering, Tezpur University in partial fulfillment for the award of the degree of Doctor of Philosophy in Electronics and Communication Engineering is a record of research work carried out by **Mr. Sujay Routh** under my supervision and guidance.

All help received by him from various sources have been duly acknowledged.

No part of this thesis has been submitted elsewhere for award of any other degree.


16/10/2024

(Supervisor)

Dr. Ratul Kumar Baruah
Associate Professor
Department of ECE
School of Engineering, Tezpur University

Declaration

I, **Sujay Routh**, hereby declare that the present thesis, entitled “**Exploring the Reliability of LDMOS and Junctionless FETs in Harsh Environments: High-Temperature and High-Radiation Applications**”, is the record of work done by me under the supervision of Dr. Ratul Kumar Baruah, Associate Professor, Department of Electronics and Communication Engineering, Tezpur University, Tezpur. The contents of the thesis represent my original works that have not been previously submitted for any Degree/Diploma/Certificate in any other University or Institutions of Higher Education.

This thesis is being submitted to Tezpur University for the Degree of Doctor of Philosophy in Electronics and Communication Engineering.

Place: Tezpur University, Tezpur

Date: 16th October 2024

Sujay Routh
(Sujay Routh)



TEZPUR UNIVERSITY

(A Central University Established by an Act of Parliament)
Napaam, Tezpur-784028, Sonitpur, Assam, India

Certificate

This is to certify that the thesis entitled, “**Exploring the Reliability of LDMOS and Junctionless FETs in Harsh Environments: High-Temperature and High-Radiation Applications**”, submitted to the School of Engineering, Tezpur University in partial fulfillment for the award of the degree of Doctor of Philosophy in Electronics and Communication Engineering is a record of research work carried out by **Mr. Sujay Routh** under my supervision and guidance.

All help received by him from various sources have been duly acknowledged.

No part of this thesis has been submitted elsewhere for award of any other degree.

(Supervisor)

Dr. Ratul Kumar Baruah
Associate Professor
Department of ECE
School of Engineering, Tezpur University



TEZPUR UNIVERSITY

(A Central University Established by an Act of Parliament)
Napaam, Tezpur-784028, Sonitpur, Assam, India

Certificate of the External Examiner

This is to certify that the thesis entitled “**Exploring the Reliability of LDMOS and Junctionless FETs in Harsh Environments: High-Temperature and High-Radiation Applications**” submitted by **Mr. Sujay Routh**, Department of Electronics & Communication Engineering, School of Engineering, Tezpur University in partial fulfilment for the award of the degree of Doctor of Philosophy in Electronics & Communication Engineering has been examined by us on _____ and found to be satisfactory.

The committee recommends for the award of the degree of Doctor of Philosophy.

Supervisor

(Dr. Ratul Kumar Baruah)

External Examiner

()

Date: _____

Date: _____

Acknowledgment

First and foremost, I express my deepest gratitude to my esteemed supervisor, Dr. Ratul Kumar Baruah, for his unwavering support, expertise, and mentorship. His encouragement, insightful feedback, and patience have been instrumental in shaping the direction of this research and in fostering my growth as a scholar.

I extend my heartfelt appreciation to the members of my thesis committee, Prof. Santanu Sarmah and Prof. Partha Pratim Sahu, for their valuable insights, constructive critiques, and thoughtful suggestions. I am thankful to Dr. Rupam Goswami, Assistant Professor at Tezpur University, for his support; his technical expertise and insightful discussions have significantly enriched shaping the trajectory of this thesis. I am also thankful to Dr. Bikram Kishore Mahajan, Reliability Engineer at Texas Instruments, United States for insightful technical discussions. Their rigorous examination and insightful comments have significantly enhanced the quality of this work. I am immensely grateful to all the individuals and institutions that have contributed to the completion of this doctoral thesis. Their support, guidance, and encouragement have been invaluable throughout this journey.

I am thankful to Tezpur University for providing me with the necessary resources, research facilities, and a stimulating academic environment that enabled me to conduct this research effectively. I extend my heartfelt appreciation to the lab technician and staff for their invaluable support, dedication, and expertise, which significantly contributed to the success of this thesis. I am indebted to the participants of my study, whose voluntary contribution and cooperation made this research possible. Their openness and willingness to share their experiences and knowledge have added depth and authenticity to this thesis.

I would like to express my gratitude to my family for their unconditional love, unwavering support, and understanding throughout my academic journey. Their belief in my abilities has been a constant source of motivation and strength. I am grateful to my friends and colleagues for their camaraderie, encouragement, and countless stimulating discussions. Their diverse perspectives have broadened my horizons and enriched my research.

My sincere thanks go to my amazing friends and lab partners, whose cooperation and support have been crucial to finishing my thesis successfully. Your combined efforts have produced a stimulating and motivating atmosphere that has greatly improved the caliber of this study. My lab partners, Albert, Ananya, Abhijit, Deepjyoti, Kakoli, Supriya, Dorothy and Yaheya deserve special recognition. Your commitment to the common goals of our study, your attitude of cooperation, and your readiness to share expertise have been helpful. Our lab's synergy has been a driving force, creating an atmosphere that encourages creative problem-solving and inventive thinking. In the midst of the scholastic difficulties, your steadfast friendship has brought me happiness and comfort, my dear friends Amarprit, Biswa, Satya Da, Bidyut, Uddipan, Ritayan, Arpita, Suhriday, Geetartha, Ankur, Monalisha, Sita, Dimpi and Deepamoni. Thanks to your support and mutual amusement, the study process has become not just manageable but joyful.

I would like to acknowledge the financial support provided by AICTE, as National Doctoral Fellow (NDF), which made it possible for me to pursue my doctoral studies.

Last but not least, I extend my heartfelt appreciation to all those whose names may not be mentioned here but have played a role in my academic and personal development. Completing this thesis would not have been possible without the combined efforts and support of all these individuals and institutions, and I am deeply grateful for their contributions, who bestowed all his blessings on me.

Sujay Routh

Dedicated to my

Parents.....

List of Figures

Fig. 1.1: Revolution to industry 5.0.....	2
Fig. 1.2: Transistor counts doubling every two years against introduction dates according to Moore's Law.....	3
Fig. 1.3: Block diagram of an n-channel MOSFET.....	4
Fig. 1.4: Schematic representation of a Si MOSFET scaled by factor k.....	5
Fig. 1.5: Channel length modulation.....	6
Fig. 1.6: Schematic of LDMOS.....	11
Fig. 1.7: Cross sectional view of a DG-SiCJLT.....	12
Fig. 1.8: Comparison between conventional MOSFET and TFET.....	13
Fig. 1.9: (a) Cross section view of n- channel JL-TFET (b) Band diagram of JL-TFET [62].....	14
Fig. 1.10: Device simulation tool flow using Sentaurus TCAD [64].....	15
Fig. 1.11: (a) Energy band diagram of a MOSFET with positive gate bias represent how ionizing radiation affects carrier generation, transport, and trapping. (b) Changes in an n-channel MOSFET (nMOS) threshold voltage after radiation exposure [69, 71].....	18
Fig. 2.1: Basic structure of the n-channel LDMOS.....	30
Fig. 2.2: (a) Schematic diagram of the LDMOS [25]. (b) Band diagram (pre-radiation) along the channel at $V_{DS} = 5V$, $T_{OX} = 20$ nm, $L_{ch} = 300$ nm and $L_{drift} = 350$ nm.....	31
Fig. 2.3: Calibration without and with radiation (0.5MRad and 1.8MRad) for $T_{OX} = 20$ nm, $L_{ch} = 300$ nm and $L_{drift} = 350$ nm and $V_{DS} = 50mV$	34
Fig. 2.4: (a) Electron-hole pair (EHP) generation profile (b) Specific ON resistance ($R_{ON,sp}$) (c) Breakdown voltage (V_{BD}) with D. $T_{OX} = 20$ nm, $L_{ch} = 300$ nm and $L_{drift} = 350$ nm.....	35
Fig. 2.5: Transfer characteristics at $V_{DS} = 1V$ (b) Surface potential (ϕ_S) at $V_{GS} = 1V$, $V_{DS} = 1V$ (c) threshold voltage (V_{TH}) and with radiation dose (R_{dose}) at $T_{OX} = 20$ nm, $L_{ch} = 300$ nm and $L_{drift} = 350$ nm and $V_{DS} = 0.05V, 1V, 2V, 4V$ and $6V$	39

Fig. 2.6: (a) Interface trap charges and (b) bulk trap charges with radiation dose (R_{dose}) at $T_{OX} = 20$ nm, $L_{ch} = 300$ nm and $L_{drift} = 350$ nm and $V_{DS} = 1$ V.....	40
Fig. 2.7: (a) Output characteristics (b) output resistance and (c) change in output resistance with TID at $T_{OX} = 20$ nm, $L_{ch} = 300$ nm and $L_{drift} = 350$ nm and $V_{DS} = 1$ V.....	41
Fig. 2.8: (a) Transconductance, G_M (b) gate to source capacitance, C_{GS} (c) gate to drain capacitance, C_{GD} and (d) unity gain cut-off-frequency, f_T with TID for $T_{OX} = 20$ nm, $L_{ch} = 300$ nm, $L_{drift} = 350$ nm, $V_{DS} = 1$ V and input frequency, $f_i = 1$ MHz.....	43
Fig. 2.9: (a) Transfer characteristics (b) f_T (c) V_{BD} (d) V_{TH} of LDMOS with Temperature at Radiation dose 1Mrad.....	45
Fig. 2.10: (a) Total Gate Capacitance (C_{GG}) (b) f_T at $V_{DS} = 1$ V, $D = 1$ Mrad with temperature.....	47
Fig. 2.11: Low-frequency noise density with TID at $T_{OX} = 20$ nm, $L_{ch} = 300$ nm and $L_{drift} = 350$ nm and $V_{GS} = V_{DS} = 1$ V.....	48
Fig. 2.12: Gaussian distribution of traps in the oxide/semiconductor interface...	49
Fig. 2.13: Low-frequency noise with (a) acceptor-like trapping concentration (b) donor-like trapping concentration and with “energy sig” at the interface of oxide/channel region for (c) acceptor-like trap (d) donor-like trap at $T_{OX} = 20$ nm, $L_{ch} = 300$ nm and $L_{drift} = 350$ nm and $V_{GS}, V_{DS} = 1$ V.....	50
Fig. 2.14: Transfer characteristics at 1Mrad of radiation dose (a) with channel doping concentration at $T_{OX} = 20$ nm, $L_{ch} = 300$ nm and $L_{drift} = 350$ nm (b) with channel length and drift length at $T_{OX} = 20$ nm (c) with oxide thickness at $T_{OX} = 20$ nm, $L_{ch} = 300$ nm, $L_{drift} = 350$ nm and $V_{DS} = 1$ V.....	53
Fig. 2.15: (a) Schematic of LDMOS with the P^+ pocket region, (b) transfer characteristics with different pocket lengths, and (c) transfer characteristics with pocket doping concentration inside the channel near the source at $T_{OX} = 20$ nm, $L_{ch} = 300$ nm, $L_{drift} = 350$ nm, $V_{DS} = 50$ mV and radiation dose = 1Mrad.....	55
Fig. 2.16: (a) Circuit diagram of CMOS inverter using LDMOS (b) Voltage transfer characteristics with TID and (c) Voltage transfer characteristics with temperature.....	56

Fig. 2.17: (a) Circuit diagram of single-stage amplifier using LDMOS (b) Output characteristics with TID (c) Output characteristics with temperature.....	57
Fig. 3.1: Schematic of an n-channel nanowire transistor.....	67
Fig.3.2: Illustrated Procedure for Fabricating NWJLFETs : (a) Ion implantation of SOI film, (b) Defining the nanowire channel, (c) Forming contact pads for the source and drain, (d) Growing or depositing the gate oxide layer, (e) Deposition of the gate metal, (f) Defining the gate electrode, (g) Examining the fabricated NWJLFET through a cross-sectional TEM image, and (h) Observing the fabricated nanowire metal-oxide-semiconductor field-effect transistor (NWMOSFET) through a bird's-eye SEM image.....	68
Fig. 3.3: Calibrated TCAD simulation with the (a) experimental device of (b) transfer characteristics (c) output characteristics for $T_{OX}(\text{SiO}_2)=3\text{ nm}$, $N_D=10^{17}\text{ cm}^{-3}$, $N_{\text{source,drain}}=9\times 10^{17}\text{ cm}^{-3}$, $T_{\text{SiC}}=1.2\text{ }\mu\text{m}$, $L=20\text{ }\mu\text{m}$	72
Fig. 3.4: Block diagram (a) SiCJLT (without the P+ layer in the oxide region) and (b) P+-SiCJLT.....	73
Fig. 3.5: Energy band diagram of P ⁺ -SiCJLT at $V_{DS} = 0,0.5V, 1V, 2V 5V, 10V$ and $V_{GS} = 0V$	74
Fig. 3.6: Transfer characteristics of P ⁺ -SiCJLT for $N_{P+} = 10^{15}, 10^{16}, 10^{17}, 10^{18}, 5 \times 10^{18}$, and 10^{19} cm^{-3} and $T_{P+} = 2\text{ nm}$, $L = 100\text{ nm}$. This is compared with equivalent dimension SiCJLT at $T_{OX} = 4\text{ nm}$. The inset of Fig. 4 shows the transconductance for the devices.....	77
Fig. 3.7: E-density at $V_{DS} = 0V$ for (a) SiCJLT at $V_{GS} = -1.5V, -0.5V, 0V$, and (b) P ⁺ -SiCJLT at $V_{GS} = 0V, 0.5V$ and $N_{P+} = 10^{18}\text{ cm}^{-3}$ for the same device dimensions as Fig. 3.4.....	78
Fig. 3.8: P ⁺ -SiCJLT is simulated with $N_{P+} = 10^{18}\text{ cm}^{-3}$, and $T_{P+} = 2\text{ nm}$ for (a) I_{DS} with gate voltage for $\text{WF}=4.1\text{-}5.1\text{ eV}$. Inset of this Fig. also shows the V_{TH} change with WF (b) V_{TH} change with N_{P+} (c) V_{TH} change with $T_{OX1} = T_{OX2} = 1\text{ to }2\text{ nm}$ (d) V_{TH} change with $T_{P+} = 1\text{ to }3\text{ nm}$. The characteristics are compared with equivalent dimension SiCJLT.....	79
Fig. 3.9: Drain current with drain voltage for P ⁺ -SiCJLT for $N_{P+} = 10^{15}\text{ cm}^{-3}, 10^{16}\text{ cm}^{-3}, 10^{17}\text{ cm}^{-3}, 10^{18}\text{ cm}^{-3}, 5 \times 10^{18}\text{ cm}^{-3}, 10^{19}\text{ cm}^{-3}$ at $T_{P+} = 2\text{ nm}$. This is compared with equivalent dimension SiCJLT.....	80
Fig. 3.10: Electron mobility for P ⁺ -SiCJLT at $T = 300\text{K} - 600\text{K}$ at 50K step size and $N_{P+} = 10^{18}\text{ cm}^{-3}, T_{P+} = 2\text{ nm}$	82

Fig. 3.11: Transfer characteristics and (b) output characteristics P ⁺ -SiCJLT at T = 300K to 600K at 50K step size for N _{P+} = 10 ¹⁸ cm ⁻³ , T _{P+} = 2nm & compared with equivalent SiCJLT.....	83
Fig. 3.12: (a) f _T with V _{GS} and (b) intrinsic gain with V _{GS} for P ⁺ -SiCJLT at T = 300K – 600K at 50K step size for N _{P+} = 10 ¹⁸ cm ⁻³ , T _{P+} = 2nm. This is compared with equivalent dimension SiCJLT.....	84
Fig. 3.13: Block diagram of SD _{Pocket} -SiCJLT with P+ pocket thickness on 5nm.....	86
Fig. 3.14: I _{ON} /I _{OFF} ratio comparison of P ⁺ -SiCJLT at N _{P+} = 10 ¹⁸ cm ⁻³ , T _{P+} = 2nm, with equivalent SiCJLT (T _{OX} = 4nm), and, SD _{Pocket} -SiCJLT (pocket width of 5 nm and T _{OX} = 4nm).....	86
Fig. 3.15: (a)-(k) Fabrication steps of a P ⁺ -SiCJLT.....	88
Fig. 4.1: Cross-sectional view of a conventional n channel (a) MOSFET (b) TFET (c) JL-TFET.....	98
Fig. 4.2: Energy band diagram of JL-TFET at fixed drain bias V _{DS} = 1V, in the ON-state (V _{CG} = 1V) and OFF-state (V _{CG} = 0V).....	99
Fig. 4.3: Formation of traps in gate oxide layer of TFET.....	101
Fig. 4.4: Schematic of (a) JL-TFET and (b) p-i-n SOI-TFET.....	102
Fig. 4.5: Energy band diagram of (a) JL-TFET and (b) p-i-n SOI TFET at a fixed drain bias V _{DS} = 1V, in the ON-state (V _{GS} = 1V) and OFF-state (V _{GS} = 0V) at T=300K.....	104
Fig. 4.6: Calibration of the simulation set-up with simulation dataset [34] for gate length L _{GC} = 20 nm, thickness T _{Si} = 5nm, Oxide (HfO ₂) thickness T _{OX} = 2 nm and doping n-type concentration of 1 × 10 ¹⁹ cm ⁻³	105
Fig. 4.7: Threshold Voltage with Temperature for JL-TFET and p-i-n SOI-TFET for T _{OX} = 2nm, L _{CG} = 20nm and V _{DS} = 1V.....	106
Fig. 4.8: (a) G _M (b) C _{GG} Variation with Temperature at fixed V _{DS} = 1V, L _{CG} = 20 nm, T _{Si} = 10 nm, T _{OX} = 2 nm.....	107
Fig. 4.9: (a)f _T (b) GBW vs gate bias voltage for both devices at V _{DS} = 1V, L _{CG} = 20 nm, T _{Si} = 10 nm, T _{OX} = 2 nm.....	108

Fig. 4.10: (a)Transfer characteristics with temperature for JL-TFET and p-i-n SOI-TFET at $V_{DS} = 1V$ $L_{CG} = 20 nm$, $T_{Si} = 10 nm$, $T_{OX} = 2 nm$ (b) BTBT profile with temperature for both JL-TFET and p-i-n SOI-TFET at $V_{GS} = 1V$ and $V_{DS} = 1V$	109
Fig. 4.11: (a) Schematic diagram for dual gate material JL-TFET, (b) BTBT contour for the dual control gate material $\phi_{M2} = 4 eV$ and $\phi_{M2} = 4.25 eV$ at $V_{GS} = -0.1V$, (c) Energy Band diagram variation of ϕ_{M2} at $V_{GS} = 0V$ (OFF-State condition), (d) Transfer characteristics with work function of the material near the fixed gate at T=300K.....	113
Fig. 4.12: (a) Transfer characteristics curve for both p-i-n TFET and JL-TFET for 300K (b) Hot electron injection curve for both p-i-n TFET and JL-TFET for 300K (c) Gate leakage characteristics curve for both p-i-n TFET and JL-TFET with variation in temperature from 300K to 500K (d) SRH-Recombination curve for both p-i-n TFET and JL-TFET for 300K.....	115
Fig. 4.13: Interface trapped charge density with time under negative bias condition.....	117
Fig. 4.14: V_{TH} degradation under negative bias conditions.....	118
Fig. 4.15: Transfer characteristics of (a) JL-TFET and (b) p-i-n SOI-TFET at $V_{DS} = 1V$ (c) V_{TH} and (d) ΔV_{TH} of JL-TFET and p-i-n SOI-TFET with TID....	119
Fig. 4.16: Radiation generation profile of JL-TFET and p-i-n SOI-TFET with radiation.....	120
Fig. 4.17: Transfer characteristics of JL-TFET with (a) oxide thickness and (b) substrate thickness for a radiation dose of 1MRad at $V_{DS} = 1V$	121
Fig. 4.18: Gaussian distribution trap in the oxide-semiconductor interface.....	122
Fig. 4.19: Trap transfer characteristics curve for drain current versus gate-to-source voltage for different peak density concentrations for different temperatures (a) acceptor-like traps, (b) donor-like traps.....	123
Fig. 4.20: Trap transfer characteristics curve for drain current versus gate-to-source voltage for different variations in Gaussian peak location for different temperatures (a) acceptor-like traps, (b) donor-like traps.....	124
Fig. 4.21: Trap transfer characteristics curve for drain current versus gate-to-source voltage for various standard deviations on Gaussian-like traps for different temperatures (a) acceptor-like traps, (b) donor-like traps.....	125

List of Tables

Table 3.1: Performance comparison of SiCJLT, $sd_{\text{pocket-sicjlt}}$, P^+ -sicjlt.....	85
Table 4.1: Parameter of nonlocal path band-to-band tunneling.....	105
Table 4.2: Electrical Parameters for Variation in Temperatures of JL-TFET and p-i-n SOITFET.....	111

Nomenclature

Symbols:

V_{TH}	Threshold Voltage
G_M	Transconductance
f_T	cut-off frequency
R_0	Output Resistance
R_{dose}	Radiation Dose
V_{DS}	Drain to Source Voltage
V_{GS}	Gate to Source Voltage
I_{DS}	Drain Current
N_{it}	Interface Trap Charges
N_{ot}	Bulk Trap Charges
V_{BD}	Breakdown Voltage
$R_{ON,sp}$	Specific ON-Resistance
q	Charge of an Electron
τ	Carrier Lifetime
ρ	Space Charge Density
m	Mass of an Electron
T	Temperature
φ_S	Surface Potential
I_{ON}	ON-State Current
I_{OFF}	OFF-State Leakage Current

I_{output}	Output Current
g_0	Number of EHP Generated Per Unit Dose
C_{GD}	Gate-to-Drain Capacitance
C_{GS}	Gate-to-Source Capacitance
C_{GG}	Total Gate Capacitance
D_{it}	density of interface traps density
D	Absorbed Radiation Dose
ϕ_f	Bulk Potential
ϕ_{ms}	Metal Workfunction
Q_{ox}	Oxide Charge Density
C_{ox}	Oxide Capacitance
V_{T0}	Threshold Voltage at Ambient Temperature
ϕ_{M1}	Metal 1 Work Function
ϕ_{M2}	Metal 2 Work Function
E_g	Band Gap
T_{OX}	Oxide Thickness
L_G	Gate Length
L_{CG}	Length of Control Gate
L_{ch}	Length of the Channel Region
L_{drift}	Length of Drift Region
Γ	Transmission Coefficient
g_v	the valley degeneracy factor

P_{ins}	The Probability of Electrons Moving Without Scattering
m_{ins}	The Effective Mass of The Insulator
v	The Magnitude of Electron Velocity
ΔV_{TH}	Threshold Voltage Shift
ΔL	Change in Length
σ_n	Capture Cross-Section of Electron
σ_p	Capture Cross-Section of Hole
v_{th}^n	Thermal Velocity of Electron
v_{th}^p	Thermal Velocity of Hole

Abbreviation:

D	Total Absorbed Dose
E	Electric Field
SS	Sub Threshold Slope
CG	Control Gate
FG	Fixed Gate
CB	Conduction Band
VB	Valance Band
NW	Nanowire
FD	Fully Depleted
RF	Radio Frequency
SH	Self-Heating
WF	Work Function
LS	Spacer Length

JLT	Junctionless Transistor
FET	Field-Effect Transistor
WBG	Wide Bandgap
TAT	Trap-Assisted Tunneling
SRH	Shockley-Read-Hall Recombination
RTN	Random Telegraph Noise
GBW	Gain Bandwidth Product
EHP	Electron Hole Pair
BTBT	Band-to-Band Tunneling
HTFET	Heterojunction Tunnel FET
MOSFET	Metal-Oxide-Semiconductor FET
JL-TFET	Junctionless Tunnel Field Effect Transistor
MugFETs	Multi-Gate FETs
ULSI	Ultra-Large-Scale Integration
DG-JLT	Double-Gate Junctionless Field-Effect Transistor
DG-SiCJLT	Dual-Gate Silicon Carbide Junctionless Transistor
SOA	Safe Operating Area
DTCO	Design Technology Co-Optimization
ZTC	Zero Temperature Coefficient
GAA	Gate All Around
ITRS	International Technology Roadmap for Semiconductors
HPC	High-Performance Computing
IoT	Internet of Things
SiO ₂	Silicon Dioxide
HfO ₂	Hafnium Dioxide

SiC	Silicon carbide
GaN	Gallium Nitride
TPU	Tensor Processing Units
VHF	Very High Frequency
UHF	Ultra-High Frequency
RESURF	Reduced Surface Field
DeMOS	Drain-extended MOS Transistor
TCAD	Technology Computer-Aided Design
BTI	Bias Temperature Instability
TDDDB	Time-Dependent Dielectric Breakdown
NBTI	Negative Bias Temperature Instability
CMOS	Complementary Metal Oxide Semiconductor
EOT	Effective Oxide Thickness
GIDL	Gate-Induced Drain Leakage